

<https://doi.org/10.1038/s41522-025-00811-w>

The microbiome is associated with obesity-related metabolome signature in the process of aging

Dana Binyamin¹, Sondra Turjeman¹, Nofar Asulin¹, Ron Schweitzer^{1,2} & Omry Koren^{1,3}✉

Aging involves changes in the gut microbiome impacting health and longevity; however, the roles of specific microbial metabolites remain understudied. Here, we examine the microbial contribution to the metabolic profile in aged mice. Fecal samples were collected from female Swiss-Webster mice raised conventionally (Conv) or germ free (GF), at 8 weeks (young) and 18 (aged) months of age, and the microbiome and metabolome were characterized. Significant differences were observed in bacterial composition and its predicted functional activity between young and aged mice. Interestingly, we found more age-related differences in metabolite abundances among Conv mice than GF mice, highlighting the contribution of the microbiome to aging. Moreover, microbiome-associated metabolites, predominantly lipids, were higher in aged mice, with linoleic acid metabolism enriched in this group. Our study underscores a microbiome-dependent component to age-related metabolic changes in mice, particularly in lipid-associated pathways, and contributes to the growing body of literature linking gut microbiota to host metabolism in aging.

Aging is a complex biological process characterized by a progressive decline in physiological function, ultimately leading to increased morbidity and mortality due to various diseases¹. Among many factors that affect the aging process, a central player is the gut microbiome², a diverse community of microorganisms residing within the gastrointestinal tract responsible for a range of interactions that affect the host's health and longevity³. One of the hallmarks of aging is the dynamic reshaping of the gut microbiome, characterized by shifts in microbial diversity^{4–6}. Some specific changes associated with aging include reduced alpha diversity, as well as reductions of beneficial taxa like *Lactobacillus* and *Bifidobacterium*^{7–9}, which can lead to compromises in gut barrier integrity and immune modulation. There are also reports of increased opportunistic pathogens like some species of the family Enterobacteriaceae¹⁰, which may contribute to systemic inflammation and age-related diseases. Because lifestyle changes, dietary patterns, age-related diseases, medications, and hospitalization can influence gut microbiome composition, and because these factors are both prevalent and dynamic among the elderly, it is often challenging to disentangle aging-specific effects from those driven by comorbidities^{11,12}. Accordingly, studies on the microbiome in older adults have reported both age-associated changes in microbial taxa and functions as well as disease-specific microbiome alterations¹³. Experimental animal models offer insights into understanding the effects of aging while minimizing the effects of environmental exposures on the gut microbiome. Several studies have examined changes in the gut

microbiome associated with aging in mice and revealed a unique gut microbial composition along with structural shifts between young and aged mice, similar to some alterations observed in human studies^{14–16}. One example of a conserved change across species is the decline in *Lactobacillus* with age^{16,17}.

While microbial metabolite production and degradation are the main modes of host-microbe interactions^{3,18}, other mechanisms, such as immune modulation, epithelial signaling, effects on gut barrier integrity, epigenetic changes, neurotransmitter production, and neuroendocrine signaling, also play an important role in mediating host physiology and are likely involved in the microbiome-host aging axis^{19–23}. It is increasingly clear that microbial metabolites serve as key mediators between the microbiota itself and associated host states. Specifically, the gut microbiota plays a crucial role in the synthesis of essential metabolites, including vitamins, amino acids, short-chain fatty acids (SCFAs), and other bioactive molecules, through various enzymatic activities and metabolic pathways²⁴. These microbially derived metabolites contribute to food digestion, xenobiotic metabolism, and the formation of diverse bioactive molecules²⁵. Metabolomic analysis enables the detection of numerous metabolites within a tissue or matrix, providing valuable biological information that might contribute to elucidating metabolic pathways influenced by aging. Several studies have characterized the metabolome in common human diseases, particularly age-related conditions like cancer²⁶, Parkinson's disease²⁷, Alzheimer's disease²⁸, chronic

¹Azrieli Faculty of Medicine, Bar-Ilan University, Safed, Israel. ²MIGAL - Galilee Research Institute, Kiryat Shmona, Israel. ³Kyung Hee University, Seoul, Republic of Korea. ✉e-mail: omry.koren@biu.ac.il

kidney disease²⁹, and diabetes³⁰, revealing alterations between healthy individuals and patients. In patients with Alzheimer's disease, SCFAs were reduced and tryptophan metabolism was altered²⁸. A similar pattern was found among those with type 2 diabetes: patients exhibited reduced SCFAs as well as disruptions in bile acid metabolism³⁰. As with the gut microbiota, many variables can affect the metabolome throughout life. The serum metabolome of aged humans has been examined in several studies^{31–33}. In the Chinese Guangxi Longevity Cohort, consisting of individuals aged 22 to 111 years, researchers observed an age-related link between the gut microbiome and serum metabolites, such as an increase in bile salts and decreased amino acids with aging³¹. In mice, Brown et al. found significant differences in metabolite profiles, such as a decrease in glutamine and histidine, across several organs at 3, 8, and 12 weeks of age, which were attributed to the microbiome³⁴. In general, few studies examined the correlation between the gut microbiome and metabolite profile in advanced aging, and to our knowledge, none have looked at the fecal metabolites, which represent gut microbiome-associated metabolites, at later stages of life.

In this study, we initially investigated microbiome changes in young (8 weeks old) and aged (18 months old) conventionally raised (Conv) mice and predicted alterations in metabolic pathways based on sequenced bacteria (Fig. 1A). Additionally, we profiled the metabolomes of germ-free (GF) mice and mice treated with antibiotics and compared their metabolomes to Conv mice (Fig. 1B). This enabled us to identify changes in microbially-derived metabolites associated with aging, as well as age-related metabolic alterations in the absence of bacteria.

Results

The bacterial composition observed in aged mice is different than that in young mice

Fecal samples were collected from young and aged Conv mice, and bacterial 16S rRNA amplicons were subsequently sequenced and compared (Fig. 1A). Significant differences were found in β -diversity (weighted UniFrac distances) between the two age groups (Fig. 2A, $p = 0.0001$). Additionally, higher bacterial richness was observed in aged mice compared to young mice (Fig. 2B, $p = 0.0007$). The taxa bar plot of the 10 most abundant genera further illustrated distinctions in the bacterial community structure between young and aged mice (Fig. 2C) and differential abundance analysis (ANCOM-BC) identified 14 genera that differed significantly between young and aged mice (Fig. 2D and Supplementary Table 2). The genera *Akkermansia* and *Prevotella* and an unclassified genus in the Bacteroidales family exhibited a higher log fold change in young mice whereas *Coprococcus* and *Turicibacter* were more abundant (relatively) in aged mice.

The microbiomes of aged mice and young mice have different predicted metabolic capabilities

To evaluate the bacterial functional profiles of young and aged Conv mice, we used PICRUSt2 to predict the functional capabilities of the bacterial communities. Predicted bacterial functional pathways differed between the

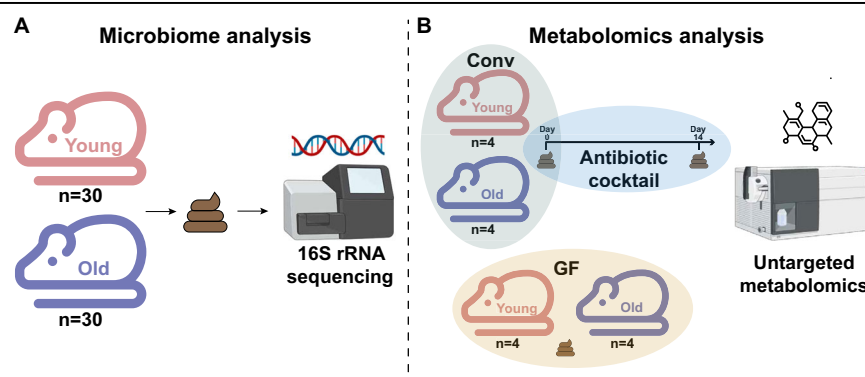
age groups (Fig. 3). The observed differences in pathway class were predominantly linked to metabolism, such as carbohydrate metabolism and lipid metabolism, that were elevated in aged mice, along with cell growth and apoptosis pathways and amino acid metabolism, that were increased in young mice.

Higher age-related metabolome variance in Conv compared to GF mice

Upon identifying differences in both the bacterial community and predicted metabolic pathways, we investigated the influence of the gut microbiome on age-related metabolite profiles. We conducted an untargeted analysis on fecal samples collected from young and aged mice raised under conventional conditions, before and after antibiotic treatment, or under GF conditions (Fig. 1B). Fecal metabolites of Conv mice clustered separately from GF mice regardless of the age of the mice (Fig. 4A; may be due in part to differences in diet, discussed below). Additionally, a noticeable separation was observed between young and aged Conv mice. Age-derived differentiation in metabolome profile was nearly absent in the GF groups in a full principal component analysis (PCA) with both Conv and GF mice, but can be seen when GF samples are analyzed separately (Fig. S1A).

With the intention of understanding the functional consequences of the different metabolite profiles between the groups, we concentrated solely on annotated compounds. To date, the majority of metabolites are unannotated; therefore, our analysis was limited to the examination of only 711 annotated metabolites. Similar to the analysis of all metabolites, the annotated metabolites clustered based on rearing conditions and age (Fig. S1B). All metabolites with significantly different concentrations ($q < 0.1$) between young and aged mice under both rearing conditions are summarized in a Venn diagram (Fig. 4B). As expected, most of the differences were observed in the young vs. aged Conv mice, with 51 annotated metabolites that showed significantly different concentrations; 14 significant annotated metabolites were observed in GF mice; and three were significantly different between the age classes in both Conv and GF mice. Significant metabolites found in the GF group and shared between the groups were attributed solely to age-related differences in mice. We further focused our investigations on the 51 differentially abundant microbially-associated metabolites identified in the Conv-young vs Conv-aged comparisons. The absence of these differences in the GF group indicates that the microbiome directly or indirectly affects the concentrations of these metabolites. These metabolites were classified into nine major groups based on their chemical classes (Fig. 4C), and lipids made up a substantial portion (29%) of the significantly differentially abundant annotated metabolites, exhibiting higher abundance in aged mice. Notably, significant variations were also observed in amino acids and peptides, nucleotides and bases, and bile acids, some of which were enriched in aged mice, and others in young mice (Fig. 4C). The 14 annotated metabolites showing significant differences between young and aged GF mice were mainly carbohydrates exhibiting elevated levels in the young GF mice compared to the aged ones (Fig. 4D, E). A summary of the metabolites that increased in aged mice in each group is given in Fig. 4E.

Fig. 1 | Experimental design. The study was divided into two main arms. **A** First, the fecal microbiome was characterized in young (8 weeks old) and old (18 months old) conventionally raised (Conv) mice using 16S rRNA gene sequencing. As germ-free (GF) mice do not harbor a microbiome, they were not included in this part of the analysis. We used in silico methods to determine predicted functionality of the characterized microbiota. **B** Untargeted metabolomics was performed on fecal samples of Conv (day 0) and GF mice. To further support our findings, we also characterized the metabolomes of young and old mice following 14 days of antibiotic treatment. Figure created using Adobe Express and BioRender.



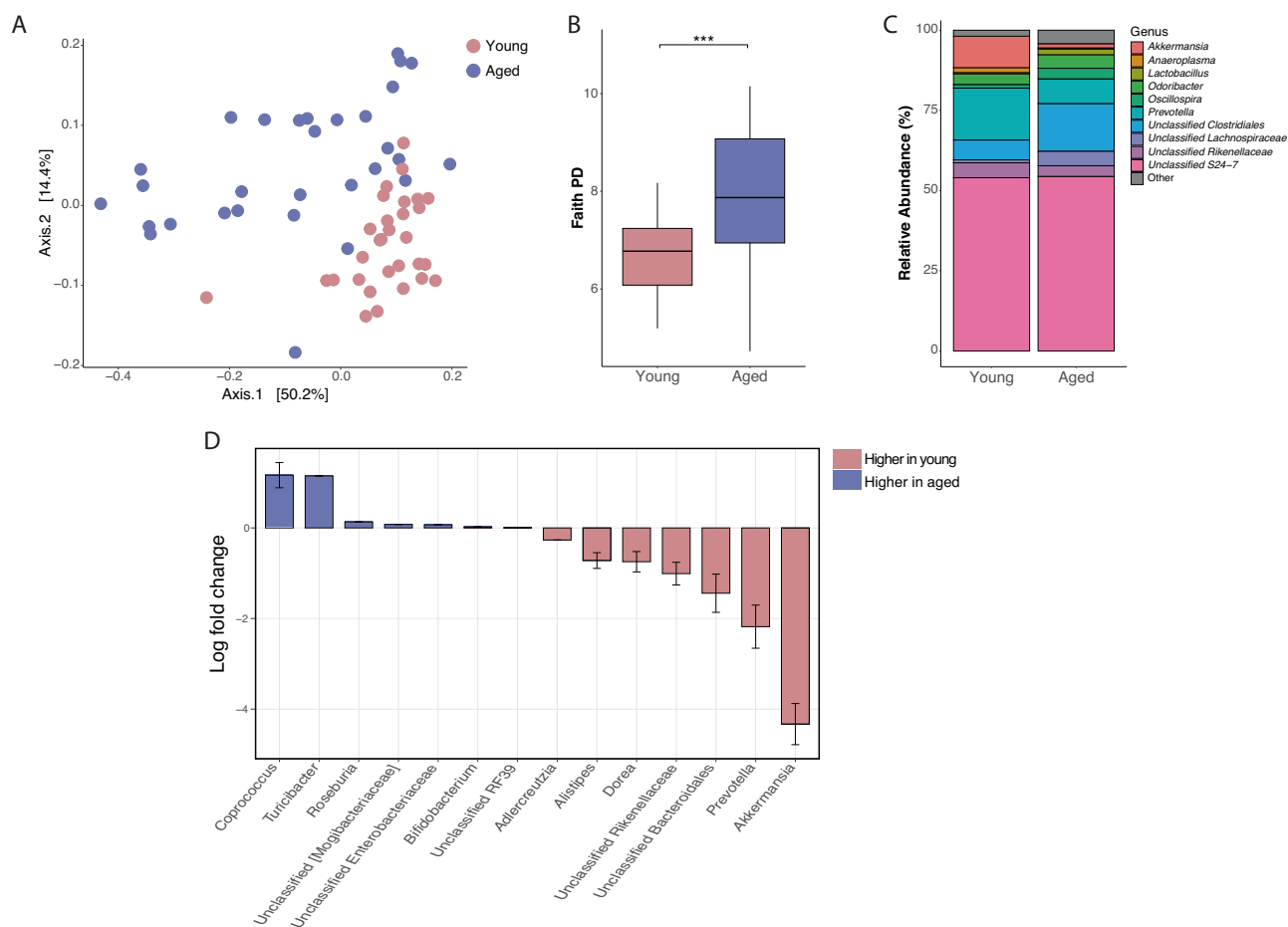


Fig. 2 | Bacterial differences between young and aged mice. A β -diversity using principal coordinate analysis (PCoA) of weighted UniFrac distances (PERMANOVA: $p = 0.0001$). **B** α -diversity based on Faith's phylogenetic diversity (PD; Mann–Whitney $p = 0.0007$). **C** Taxa bar plot of the 10 most abundant genera. **D** Log

fold change of significantly different taxa identified by analysis of microbiome composition with bias correction (ANCOM-BC). *** $q < 0.001$. $n = 30$ for each group.

Bacterial contribution to increases in linoleic acid metabolism in aged mice

Among the distinct metabolites observed between young and aged Conv mice, an increase in lipids was noted, with four of these lipids (28%) identified as components of the linoleic acid metabolism pathway. In addition, enrichment analysis detected linoleic acid metabolism as the most enriched pathway in these samples (Fig. S2A). Linoleic acid (Fig. 5A, $q = 0.04$), 9(10)-EpOM (Fig. 5B $q = 0.07$), 9-OxoODE (Fig. 5C $q = 0.08$), and 13-OxoODE (Fig. 5D, $q = 0.09$), metabolites involved in linoleic acid metabolism (Fig. 5E), were highly abundant in the aged Conv mice compared to young Conv mice. In addition, the metabolite 12R-HETE, which is also present in a higher concentration in aged Conv mice ($q = 0.04$, Fig S2B), is part of the arachidonic acid metabolism pathway, which is downstream of linoleic acid metabolism.

Given our aim to replicate a natural and normal aging state, the Conv mice were provided with a regular, non-sterilized diet as the autoclaved diet the GF mice received might result in the loss of some nutrients. To tease apart the effects of diet differences and better understand how the absence of microbiota affects host metabolome, metabolomic analysis was also conducted on Conv mice fed a non-sterile diet and administered antibiotics, and metabolites that are part of the linoleic acid metabolism pathway were examined pre- and post-treatment (Fig. 1B). Interestingly, a notable decrease in metabolite levels was observed in the aged mice following antibiotic administration, whereas no discernible effect was observed in the young mice (Fig. S3).

Discussion

Growing evidence suggests that the gut microbiome plays a central role in many age-related changes and contributes to longevity across various species³⁵. In addition, since a shift in the microbiome is one of the hallmarks of aging and a major player in health and diseases, understanding the impact of the microbiome on the host in particularly vulnerable elderly populations is important for the development of targeted therapeutic strategies. As expected, microbiome characterization of young and aged mice revealed variations in the microbiome composition across different age groups, providing valuable insights into the dynamics of microbial communities. The genus *Akkermansia*, for instance, known for its association with longevity and antidiabetic effects, decreased in aged mice^{4,36}. Also, consistent with the body of literature, the genus *Turicibacter*, which is associated with proinflammatory factors and correlated with high fat mass, was increased in aged mice^{14,37}. Analysis of predicted functional capabilities of young and aged microbiomes supported the influence of the gut bacterial population on age-associated metabolome, and most of the detected pathways were related to metabolism. Previous studies suggested that the rate of metabolic activity and its byproducts played pivotal roles in driving the aging process^{38,39}. For instance, lipid metabolism is a well-documented pathway in the literature that strongly correlates with aging, as evidenced by numerous studies highlighting significant differences in humans and mice^{40–42}. With aging, there is an increase in body fat content accompanied by alterations in lipid metabolism and associated metabolite levels. Here we also observe that aged mice weighed more than young mice (Fig. S4), regardless of whether they were reared in Conv or GF conditions. This change plays a critical role

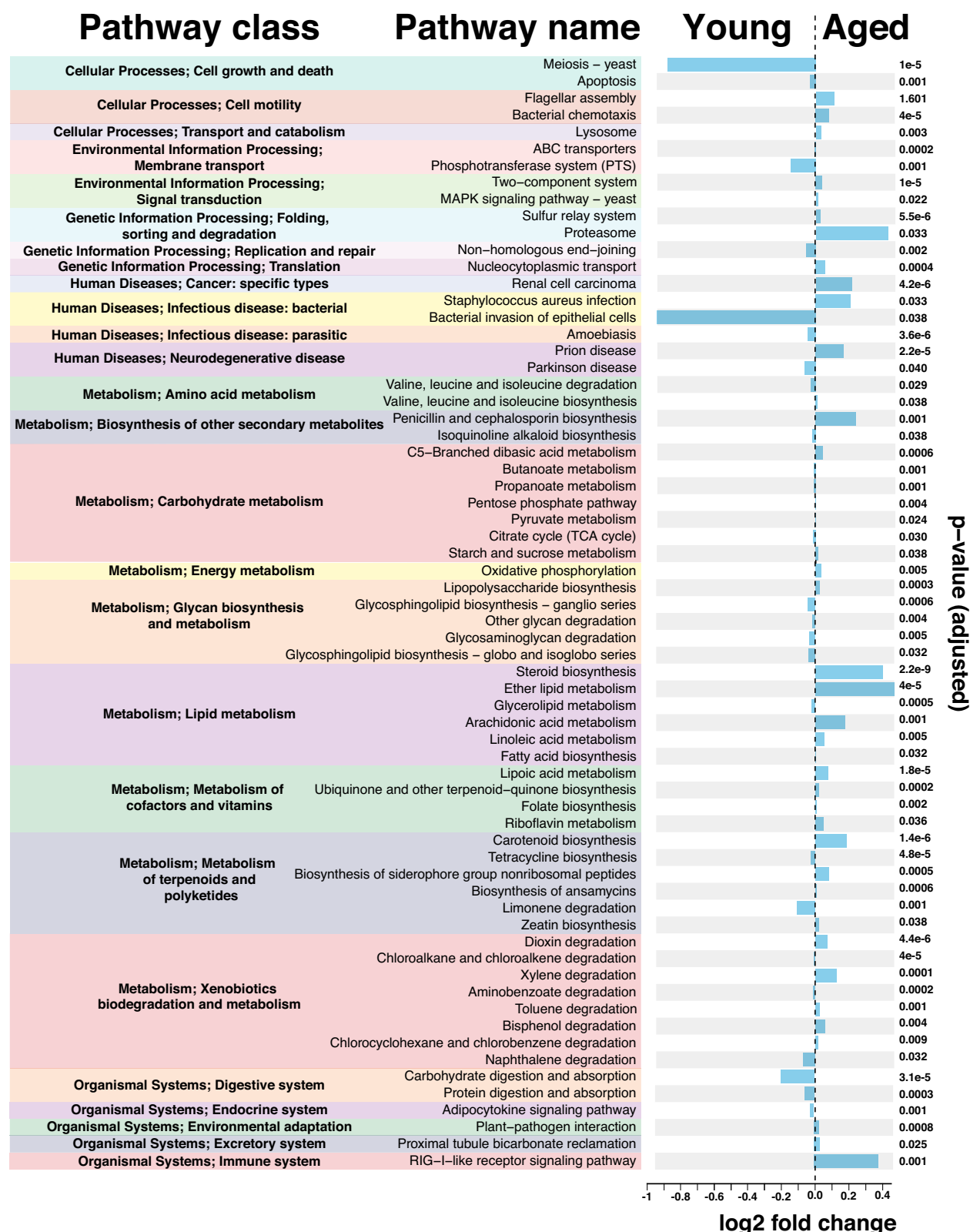


Fig. 3 | Functional pathway predictions in young and aged mice from sequenced bacteria using PICRUSt2. Bar chart of significantly different pathways between young and aged mice based on 16S rRNA gene sequence data. Metabolites are colored by pathway.

in a range of age-related diseases such as cardiovascular disorders, cancer, and Alzheimer's disease⁴⁰.

While PICRUSt2 is a widely used method for predicting microbially associated metabolites from 16S rRNA amplicon sequencing data, to fully understand the metabolic differences in our experimental groups, we

performed untargeted metabolomics profiling on a subset of samples. After demonstrating a clear separation between Conv and GF mice, we also observed different clustering between young and aged mice, mostly in the conventionally raised group. Microbiome-related differences in metabolites were categorized into nine main groups, and differences in lipids were most

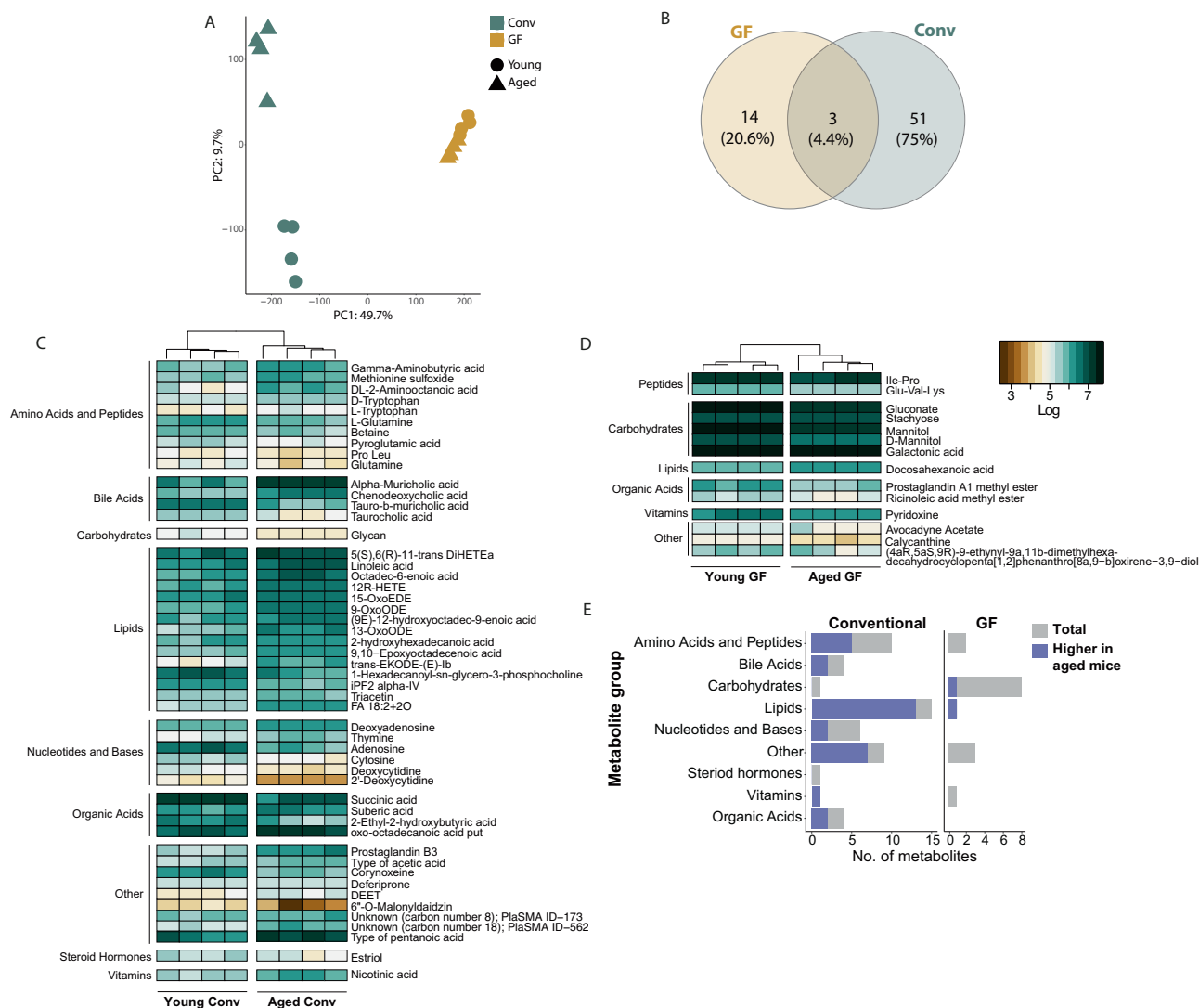


Fig. 4 | Metabolome differences between young and aged mice raised in conventional (Conv) and germ-free (GF) conditions. A Principal component analysis (PCA) of all fecal metabolites of aged and young mice raised in Conv and GF conditions. **B** Venn diagram of all significantly differentially abundant annotated

metabolites between young and aged mice (t -test, $q < 0.1$). **C** Heatmap of annotated metabolites that were significantly different between age classes in (C) the Conv and (D) the GF groups. Colors represent log₁₀ of metabolite peak intensity. **E** Summary of highly abundant metabolites in aged mice.

prominent, with increased abundance in aged mice. In a study comparing Conv and GF mice fed with a regular chow diet, an increase in several lipids was observed in the serum, adipose tissue, and liver of Conv mice, indicating the microbial effect on lipid metabolism⁴³. In contrast, in GF mice, we mainly found differences in carbohydrates and peptides between the age groups. A hallmark of aging is the decline in metabolic flexibility, characterized by an ineffective transition in utilizing fuel sources from carbohydrates to fatty acids based on their varying availability⁴⁴. Similarly, the intestinal microbiome plays a crucial role in converting non-digestible carbohydrates into metabolites⁴⁵. Our results suggest a potential contribution of the gut microbiome to this change and support a possible role for the microbiome in influencing lipid metabolism during aging.

Disruption of lipid metabolism is associated with obesity, leading to abnormalities in blood lipid levels, deposition of lipids in non-typical locations, and the onset of metabolic disorders such as non-alcoholic fatty liver disease⁴⁶. In a previous study on the effects of the microbiome in aging, we found that fecal microbiota transplantation from aged mice into young GF recipients caused an increase in several obesity parameters, including increased fat mass, food consumption, and elevated insulin levels in the blood¹⁴. Albouery et al. discovered that alterations in the gut microbiome

associated with aging may impact lipid metabolism not only in the gut but also in other organs, such as the brain and liver⁴⁷.

Furthermore, in our study, four of the lipids with significantly different concentrations were characterized as metabolites involved in the linoleic acid metabolism pathway. Linoleic acid is an essential fatty acid that has a significant role in adipocyte differentiation. An excess of arachidonic acid within cells, derived from the intake of dietary linoleic acid, has the potential to trigger adipocyte differentiation through multiple interconnected pathways⁴⁸. Excessive linoleic acid consumption has also been associated with obesity and implicated in the chronic inflammatory condition often observed in individuals with obesity^{48,49}. Members of the gut microbiome, such as *Lactobacillus*⁵⁰, *Ruminococcus*, and *Oscillospira*⁵¹, can produce linoleic acid. Here, we found that the linoleic acid metabolism pathway was predicted to be enriched in aged mice in our bacterial PICRUST2 analysis, and when examining differences in the abundances of these three specific taxa, we found higher abundance of *Lactobacillus* and *Oscillospira* in aged mice (Fig. S5, t -test).

Building upon our previous research, demonstrating that the gut microbiome of aged mice has obesogenic characteristics¹⁴, we hypothesize that alterations in the microbiome in aging increase lipids levels in feces, and likely systemically, and impact linoleic acid metabolism, which potentially

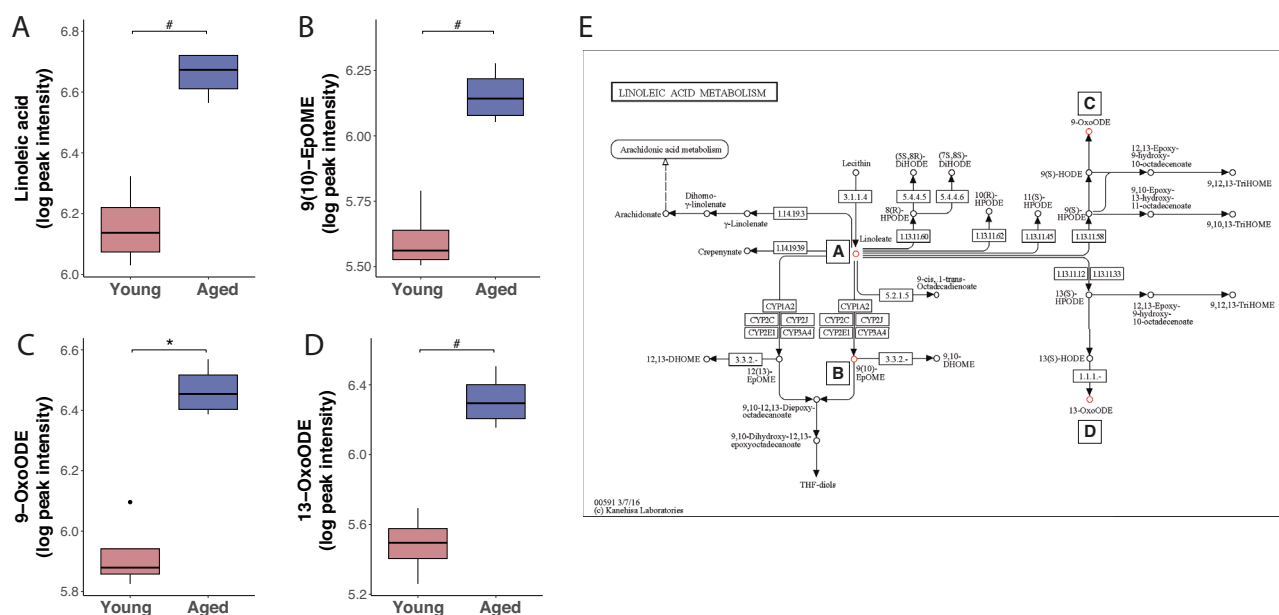


Fig. 5 | Bacterially associated elevation in linoleic acid metabolism in aged mice. A–D Peak intensity of age-related, differentially abundant metabolites that are part of linoleic acid metabolism in conventionally raised (Conv) mice: Linoleic acid,

9(10)-EpOME, 9-OxoODE, and 13-OxoODE, # $q < 0.1$, * $q = 0.04$. E Linoleic acid metabolism pathway (KEGG map00591⁷⁶).

contributes to increased obesity parameters in aged mice. We do acknowledge that aged GF mice also exhibit higher body weight compared to young GF mice, indicating that age-related weight gain can occur independently of the microbiome and is likely influenced by additional age-associated factors.

One limitation of this study is the inability to establish direct correlations between the microbiome and metabolites due to the lack of matched samples for analysis. However, the comparison to GF mice highlighted the influence of the microbiome on different metabolites. Furthermore, variations in diets, including the autoclaved diet provided to the GF mice, may have influenced our results, as dietary macronutrient composition can have an impact on the gut microbiome and subsequently, the fecal metabolome. In addition, it prevented direct comparisons between the Conv and the GF groups. To mitigate this issue, our analysis primarily focused on discerning differences between young and aged mice within each group separately. We chose not to feed the conventional group an autoclaved diet as well, as this process destroys many of the diet's components, thus hindering the simulation of the natural and healthy aging process⁵². Additionally, the exclusive use of fecal samples as opposed to serum samples limits our understanding of metabolite transport into the bloodstream, thus hindering a comprehensive assessment of systemic metabolic changes associated with the gut microbiome in aging mice. Future studies incorporating both fecal and serum metabolomics analyses could provide valuable insights into the transport dynamics of metabolites and their systemic effects. Lastly, our study focused only on female mice, as the effects of the microbiome on the metabolome in females are understudied^{53,54}. While this decision was made to address current knowledge gaps, future studies should include both sexes to better understand the potential sex-dependent differences in microbiome-metabolome interactions during aging.

Methods

Mouse handling and sample collection

Fecal samples were collected from young (8 weeks old) and old (18 months old) Conv and GF Swiss-Webster (SW) female mice. Mice were weighed at the time of fecal sample collection. In addition, following fecal sample collection, Conv mice received an antibiotic treatment consisting of 0.04 g ciprofloxacin, 0.2 g metronidazole, and 0.1 g vancomycin in 400 ml sterile

water for 2 weeks and were then sampled again. All Conv mice were housed 2–3 mice per cage in the same room, and GF mice were housed in cages of up to 4 mice per cage in sterile isolators. GF mice were fed an autoclaved chow diet enriched with proteins (28%) and fats (22%) (Altromin 1414 IRR, Lage, Germany) while Conv mice were fed a normal chow diet (11% fats, 24% proteins and 65% carbohydrates; Altromin 1324 IRR, Lage, Germany). All mice were maintained at 22 ± 1 °C with a 12 h light/dark cycle at the animal facility of Azrieli Faculty of Medicine, BIU, Israel. The experiment was performed following approval from the Institutional Animal Care and Use Committee (permit number 67-09-2021). As only fecal samples were collected, no anesthesia was used. Animals were aged further as part of an extension of this study such that no animals were euthanized in this research.

Gut microbiome characterization

Total DNA was extracted from fecal samples of 30 young and 30 aged Conv mice (Fig. 1A) using the MagMAX Microbiome Ultra Kit (Thermo Fisher Scientific, Waltham MA, USA) according to the manufacturer's instructions, following a 2-min bead-beating step (BioSpec, Bartlesville, OK, USA). Several GF fecal samples were also included to ensure the GF status. Amplification of the V4 region of the bacterial 16S rRNA gene was performed using barcoded 515 F and 806 R primers following the Earth Microbiome Project protocol⁵⁵. The PCR reaction was comprised of 2 µl of 515 F primer (10 µM), 2 µl of 806 R primer (10 µM), 25 µl of PrimeSTAR Max PCR Readymix (Takara, San Jose, CA, USA), 17 µl of ultra-pure water, and approximately 20 ng of DNA. The PCR protocol consisted of an initial step at 95 °C for 3 min, followed by 30 cycles of 10 s at 98 °C, 5 s at 55 °C, and 20 s at 72 °C, with a final elongation step for 1 min at 72 °C. Amplicons were purified using VAHTS DNA Clean Beads (Vazyme, Nanjing, China) and quantified with the Quant-iT PicoGreen dsDNA Assay Kit (Invitrogen, Carlsbad, CA, USA). Equimolar amounts of DNA from each sample were pooled to ensure consistent read depth. After gel electrophoresis on a 2% agarose E-Gel (Invitrogen, Carlsbad, CA, USA), DNA was extracted from the gel using the NucleoSpin Gel and PCR Clean-up Kit (Macherey-Nagel, Düren, Germany) before being sequenced on the Illumina Miseq platform at the Genomic Center, Azrieli Faculty of Medicine, BIU, Israel.

Bioinformatic analysis was conducted on the sequence reads using QIIME2 software (version 2023.7)⁵⁶, with error correction performed by DADA2⁵⁷. A phylogenetic tree was generated and taxonomic classification was achieved utilizing the Greengenes reference database with a confidence threshold set at 99%⁵⁸. Data was then exported from QIIME2 into R (version 4.1.2). A phyloseq object was built using the phyloseq R package (version 1.46)⁵⁹. Samples were rarefied based on rarefaction curves (vegan package, version 2.6-4⁶⁰) to a depth of 3000 sequences. While rarefying may reduce sensitivity due to data loss, it has the advantages of not being prone to false positives or effects of sequencing effort that can impact other normalization methods⁶¹. For beta diversity assessment, principal coordinate analysis (PCoA) was applied based on weighted UniFrac distances⁶². Statistical analysis was done with the *adonis2* function using the vegan package. Alpha diversity, measured by Faith's phylogenetic diversity⁶³, was also computed and compared using Mann–Whitney tests. To identify differentially abundant taxa, analysis of compositions of microbiomes with bias correction (ANCOM-BC) was performed with the ANCOM-BC package (version 2.4)⁶⁴. Since the ANCOM-BC function includes normalization, we used the unrarefied taxa table for this analysis. In addition, differences in *Lactobacillus*, *Ruminococcus*, and *Oscillospira* abundance between the groups were tested using a t-test. These taxa were specifically targeted because they were previously associated with aging in humans and mice (see lit review above) and because of their relationship with linoleic acid metabolism (all three taxa,⁵⁰). All figures were generated using ggplot2 (version 3.3.4)⁶⁵. For functional predictions based on bacterial sequencing, PICRUSt2⁶⁶ was used within the QIIME2 pipeline and then visualized results in R using the ggpict2 package (version 1.7.3)⁶⁷.

Metabolomics sample preparation

Metabolite extraction and protein precipitation were conducted by Afekta Technologies Ltd (Kuopio, Finland) on four fecal samples from each group (young and aged mice, raised conventionally, before and after antibiotics treatment, or germ free; Fig. 1B). Samples were individually homogenized with cold 80% v/v aqueous LC-MS ultra-grade methanol in a ratio of 900 μ L per 100 mg of sample using a Bead Ruptor 24 Elite homogenizer (OMNI, Kennesaw GA, USA) at 6 m/s at 2 ± 2 °C for 30 s. Following 15 min ice incubation and 10 s vortex, samples were centrifuged for 10 min at 4 °C and $17,000 \times g$. The supernatant was collected and filtered (Captiva ND filter plate 0.2 μ m, Agilent, Santa Clara, CA, USA) by centrifuging for 5 min at $700 \times g$ at 4 °C, and then samples were kept at 4 °C until analysis. Following this procedure, a portion of each sample (60 μ L) was pooled into one tube to be used as a pooled quality control sample in the analysis.

Metabolomics liquid chromatography–mass spectrometry (LC-MS) analysis

Samples were analyzed in an untargeted manner by liquid chromatography–mass spectrometry (LC-MS) on an Agilent 6546 Q-TOF LC/MS system with Agilent Jet Stream source and 1290 Infinity II UHPLC system (Santa Clara, CA, USA). The analytical method has been described in detail by Hanhineva et al.⁶⁸ and Klävis et al.⁶⁹. In brief, for the reversed-phase (RP) separation, a Zorbax Eclipse XDB-C18 column (2.1 \times 100 mm, 1.8 μ m; Agilent, Santa Clara, CA, USA) was used and an Acquity UPLC BEH amide column (Waters, Milford, MA, USA) was used for the HILIC separation. After each chromatographic run, ionization was carried out using jet stream electrospray ionization (ESI) in the positive and negative mode, yielding four data files per sample. The collision energies for the MS/MS analysis were selected as 10, 20, and 40 V, for compatibility with spectral databases.

Metabolomics data processing

Peak detection and alignment were conducted using MS-DIAL version 4.90⁷⁰. Peak collection involved inclusion of *m/z* values ranging from 50 to 1500 and all retention times, with a minimum peak height set at 3000. The peaks were detected using a linear weighted moving average algorithm. Alignment of peaks across samples employed a retention time tolerance of 0.1 min and an *m/z* tolerance of 0.015 Da. To eliminate solvent background,

blank solvent samples were utilized, with the condition that signal abundance across samples was at least five times greater than the average in the solvent blank samples to be retained for further data analysis.

After the peak picking, a total of 77,578 molecular features were included in the data preprocessing and clean-up step. The annotation of each metabolite and the level of confidence for the identification were given based on the recommendations published by the Chemical Analysis Working Group (CAWG) Metabolomics Standards Initiative (MSI)⁷¹. The final analysis was made on 711 metabolites with annotation tags of at least of 430 (Supplementary Table 1). Metabolites were classified based on metabolite type manually, and from these groups, common pathways were inferred. In addition, pathway enrichment analysis was conducted considering the 51 annotated metabolites that had significantly different concentrations across the age groups of Conv mice. This analysis was performed using the MetaboAnalyst 6.0 website⁷², to identify significantly over-represented metabolic pathways.

Metabolomics statistics and visualizations

A PCA plot was generated with the *prcomp* function (R base stats package, version 4.3.2) based on the full metabolome profile of all 77,578 metabolites and based on only annotated metabolites. Next, differences between annotated metabolite concentrations in young and aged mice were examined for Conv and GF mice separately using the peak intensities recorded for each sample for each metabolite. T-tests with FDR corrections were performed using the genefilter package (version 1.84)⁷³. A Venn diagram was generated using InteractiVenn, a web-based tool, considering all significant metabolites (young vs old, $q < 0.1$) in Conv and GF mice groups, and a heatmap was generated using the ComplexHeatmap package (version 2.18)⁷⁴ considering significantly different metabolites present in each group. Differences between linoleic acid metabolism in the antibiotic-treated mice were examined using t-tests after equal variances were confirmed. All figures were generated using the ggplot2 package unless specified otherwise⁶⁵.

Data availability

All sequencing data were submitted to EBI (project accession number ERP160940). The metabolomics data have been deposited to MetaboLights repository with the study identifier MTBLS10085⁷⁵.

Received: 17 October 2024; Accepted: 7 August 2025;

Published online: 25 August 2025

References

1. Khaltourina, D., Matveyev, Y., Alekseev, A., Cortese, F. & Ioviță, A. Aging fits the disease criteria of the international classification of diseases. *Mech. Ageing Dev.* **189**, 111230 (2020).
2. Heintz, C. & Mair, W. You are what you host: microbiome modulation of the aging process. *Cell* **156**, 408–411 (2014).
3. Boyajian, J. L., Ghebretatios, M., Schaly, S., Islam, P. & Prakash, S. Microbiome and human aging: probiotic and prebiotic potentials in longevity, skin health and cellular senescence. *Nutrients* **13**, 4550 (2021).
4. Bárcena, C. et al. Healthspan and lifespan extension by fecal microbiota transplantation into progeroid mice. *Nat. Med* **25**, 1234–1242 (2019).
5. López-Otín, C., Blasco, M. A., Partridge, L., Serrano, M. & Kroemer, G. Hallmarks of aging: an expanding universe. *Cell* **186**, 243–278 (2023).
6. Wilmanski, T. et al. Gut microbiome pattern reflects healthy aging and predicts survival in humans. *Nat. Metab.* **3**, 274–286 (2021).
7. Jing, Y. et al. Role of microbiota–gut–brain axis in natural aging-related alterations in behavior. *Front. Neurosci.* **18**, 1362239 (2024).
8. Alseigiani, A. S. & Shah, Z. A. The influence of gut microbiota alteration on age-related neuroinflammation and cognitive decline. *Neural Regen. Res.* **17**, 2407 (2022).
9. Jing, Y. et al. Age-related alterations in gut homeostasis are microbiota dependent. *npj Biofilms Microbiomes* **11**, 51 (2025).

10. Boopathi, S. et al. Gut Enterobacteriaceae and uraemic toxins - Perpetrators for ageing. *Exp. Gerontol.* **173**, 112088 (2023).
11. Bosco, N. & Noti, M. The aging gut microbiome and its impact on host immunity. *Genes Immun.* **22**, 289–303 (2021).
12. You, X., Dadwal, U. C., Lenburg, M. E., Kacena, M. A. & Charles, J. F. Murine gut microbiome meta-analysis reveals alterations in carbohydrate metabolism in response to aging. *mSystems* **7**, e01248–21 (2022).
13. Ghosh, T. S., Shanahan, F. & O'Toole, P. W. The gut microbiome as a modulator of healthy ageing. *Nat. Rev. Gastroenterol. Hepatol.* **19**, 565–584 (2022).
14. Binyamin, D. et al. The aging mouse microbiome has obesogenic characteristics. *Genome Med.* **12**, 87 (2020).
15. Barreto, H. C., Sousa, A. & Gordo, I. The landscape of adaptive evolution of a gut commensal bacteria in aging mice. *Curr. Biol.* **30**, 1102–1109.e5 (2020).
16. van der Lugt, B. et al. Integrative analysis of gut microbiota composition, host colonic gene expression and intraluminal metabolites in aging C57BL/6J mice. *Aging* **10**, 930–950 (2018).
17. Xu, C., Zhu, H. & Qiu, P. Aging progression of human gut microbiota. *BMC Microbiol.* **19**, 236 (2019).
18. Zhang, Y., Chen, R., Zhang, D., Qi, S. & Liu, Y. Metabolite interactions between host and microbiota during health and disease: which feeds the other? *Biomed. Pharmacother.* **160**, 114295 (2023).
19. Molinero, N. et al. Gut microbiota, an additional hallmark of human aging and neurodegeneration. *Neuroscience* **518**, 141–161 (2023).
20. Best, L. et al. Metabolic modelling reveals the aging-associated decline of host–microbiome metabolic interactions in mice. *Nat. Microbiol.* **10**, 973–991 (2025).
21. Nichols, R. G. & Davenport, E. R. The relationship between the gut microbiome and host gene expression: a review. *Hum. Genet.* **140**, 747–760 (2021).
22. Loh, J. S. et al. Microbiota–gut–brain axis and its therapeutic applications in neurodegenerative diseases. *Sig Transduct. Target Ther.* **9**, 1–53 (2024).
23. Zheng, D., Liwinski, T. & Elinav, E. Interaction between microbiota and immunity in health and disease. *Cell Res.* **30**, 492–506 (2020).
24. Mukhopadhyay, I. & Louis, P. Gut microbiota-derived short-chain fatty acids and their role in human health and disease. *Nat. Rev. Microbiol.* 1–17 <https://doi.org/10.1038/s41579-025-01183-w>. (2025)
25. Belizário, J. E., Faintuch, J. & Garay-Malpartida, M. Gut microbiome dysbiosis and immunometabolism: new frontiers for treatment of metabolic diseases. *Mediat. Inflamm.* **2018**, e2037838 (2018).
26. Xie, Z. et al. Metabolomic analysis of gut metabolites in patients with colorectal cancer: Association with disease development and outcome. *Oncol. Lett.* **26**, 358 (2023).
27. Yan, Z. et al. Alterations of gut microbiota and metabolome with Parkinson's disease. *Microb. Pathog.* **160**, 105187 (2021).
28. Wu, L. et al. Altered gut microbial metabolites in amnesic mild cognitive impairment and Alzheimer's disease: signals in host–microbe interplay. *Nutrients* **13**, 228 (2021).
29. Wang, H. et al. Perturbed gut microbiome and fecal and serum metabolites are associated with chronic kidney disease severity. *Microbiome* **11**, 3 (2023).
30. Al Bataineh, M. T. et al. Uncovering the relationship between gut microbial dysbiosis, metabolomics, and dietary intake in type 2 diabetes mellitus and in healthy volunteers: a multi-omics analysis. *Sci. Rep.* **13**, 17943 (2023).
31. Sun, L. et al. Age-dependent changes in the gut microbiota and serum metabolome correlate with renal function and human aging. *Aging Cell* **22**, e14028 (2023).
32. Yu, Z. et al. Human serum metabolic profiles are age dependent. *Aging Cell* **11**, 960–967 (2012).
33. Lawton, K. A. et al. Analysis of the adult human plasma metabolome. *Pharmacogenomics* **9**, 383–397 (2008).
34. Brown, K. et al. Microbiota alters the metabolome in an age- and sex-dependent manner in mice. *Nat. Commun.* **14**, 1348 (2023).
35. Badal, V. D. et al. The gut microbiome, aging, and longevity: a systematic review. *Nutrients* **12**, 3759 (2020).
36. Plovier, H. et al. A purified membrane protein from Akkermansia muciniphila or the pasteurized bacterium improves metabolism in obese and diabetic mice. *Nat. Med.* **23**, 107–113 (2017).
37. Liu, A. et al. Aging increases the severity of colitis and the related changes to the gut barrier and gut microbiota in humans and mice. *J. Gerontol. Ser. A* **75**, 1284–1292 (2020).
38. Catic, A. Cellular metabolism and aging. *Prog. Mol. Biol. Transl. Sci.* **155**, 85–107 (2018).
39. Palmer, A. K. & Jensen, M. D. Metabolic changes in aging humans: current evidence and therapeutic strategies. *J. Clin. Investig.* **132**, e158451 (2024).
40. Chung, K. W. Advances in understanding of the role of lipid metabolism in aging. *Cells* **10**, 880 (2021).
41. Feng, L. et al. Age-related trends in lipid levels: a large-scale cross-sectional study of the general Chinese population. *BMJ Open* **10**, e034226 (2020).
42. Hornburg, D. et al. Dynamic lipidome alterations associated with human health, disease and ageing. *Nat. Metab.* **5**, 1578–1594 (2023).
43. Velagapudi, V. R. et al. The gut microbiota modulates host energy and lipid metabolism in mice [S]. *J. Lipid Res.* **51**, 1101–1112 (2010).
44. Zhou, Q., Yu, L., Cook, J. R., Qiang, L. & Sun, L. Deciphering the decline of metabolic elasticity in aging and obesity. *Cell Metab.* **35**, 1661–1671.e6 (2023).
45. Rowland, I. et al. Gut microbiota functions: metabolism of nutrients and other food components. *Eur. J. Nutr.* **57**, 1–24 (2018).
46. Schoeler, M. & Caesar, R. Dietary lipids, gut microbiota and lipid metabolism. *Rev. Endocr. Metab. Disord.* **20**, 461–472 (2019).
47. Albouery, M. et al. Age-related changes in the gut microbiota modify brain lipid composition. *Front. Cell Infect. Microbiol.* **9**, 444 (2020).
48. Naughton, S. S., Mathai, M. L., Hryciw, D. H. & McAinch, A. J. Linoleic acid and the pathogenesis of obesity. *Prostaglandins Other Lipid Mediat.* **125**, 90–99 (2016).
49. Mamounis, K. J., Yasrebi, A. & Roepke, T. A. Linoleic acid causes greater weight gain than saturated fat without hypothalamic inflammation in the male mouse. *J. Nutr. Biochem.* **40**, 122–131 (2017).
50. Fujimoto, D. et al. The relationship between unique gut microbiome-derived lipid metabolites and subsequent revascularization in patients who underwent percutaneous coronary intervention. *Atherosclerosis* **375**, 1–8 (2023).
51. Shenghua, P. et al. An integrated fecal microbiome and metabolome in the aged mice reveal anti-aging effects from the intestines and biochemical mechanism of FuFang zhenshu TiaoZhi (FTZ). *Biomed. Pharmacother.* **121**, 109421 (2020).
52. Su, X. et al. High-coverage metabolome analysis reveals significant diet effects of autoclaved and irradiated feed on mouse fecal and urine metabolomics. *Mol. Nutr. Food Res.* **65**, 2100110 (2021).
53. Lee, J. et al. Gut microbiota-derived short-chain fatty acids promote poststroke recovery in aged mice. *Circ. Res.* **127**, 453–465 (2020).
54. Parker, A. et al. Fecal microbiota transfer between young and aged mice reverses hallmarks of the aging gut, eye, and brain. *Microbiome* **10**, 68 (2022).
55. Caporaso, J. G. et al. Ultra-high-throughput microbial community analysis on the Illumina HiSeq and MiSeq platforms. *ISME J.* **6**, 1621–1624 (2012).
56. Bolyen, E. et al. Reproducible, interactive, scalable and extensible microbiome data science using QIIME 2. *Nat. Biotechnol.* **37**, 852–857 (2019).
57. Callahan, B. J. et al. DADA2: high-resolution sample inference from Illumina amplicon data. *Nat. Methods* **13**, 581–583 (2016).

58. DeSantis, T. Z. et al. Greengenes, a chimera-checked 16S rRNA gene database and workbench compatible with ARB. *Appl. Environ. Microbiol.* **72**, 5069–5072 (2006).
59. McMurdie, P. J. & Holmes, S. phyloseq: an R package for reproducible interactive analysis and graphics of microbiome census data. *PLoS ONE* **8**, e61217 (2013).
60. Dixon, P. VEGAN, a package of R functions for community ecology. *J. Veg. Sci.* **14**, 927–930 (2003).
61. Weiss, S. et al. Normalization and microbial differential abundance strategies depend upon data characteristics. *Microbiome* **5**, 27 (2017).
62. Lozupone, C. & Knight, R. UniFrac: a new phylogenetic method for comparing microbial communities. *Appl. Environ. Microbiol.* **71**, 8228–8235 (2005).
63. Faith, D. P. & Baker, A. M. Phylogenetic diversity (PD) and biodiversity conservation: some bioinformatics challenges. *Evol. Bioinform. Online* **2**, 121–128 (2007).
64. Lin, H. & Peddada, S. D. Analysis of compositions of microbiomes with bias correction. *Nat. Commun.* **11**, 3514 (2020).
65. Wickham, H. *Ggplot2* (Springer International Publishing, <https://doi.org/10.1007/978-3-319-24277-4>, 2016).
66. Douglas, G. M. et al. PICRUSt2 for prediction of metagenome functions. *Nat. Biotechnol.* **38**, 685–688 (2020).
67. Yang, C. et al. ggpictur2: an R package for PICRUSt2 predicted functional profile analysis and visualization. *Bioinformatics* **39**, btad470 (2023).
68. Hanhineva, K. et al. Nontargeted metabolite profiling discriminates diet-specific biomarkers for consumption of whole grains, fatty fish, and bilberries in a randomized controlled trial1, 2, 3. *J. Nutr.* **145**, 7–17 (2015).
69. Klåvus, A. et al. notame: workflow for non-targeted LC-MS metabolic profiling. *Metabolites* **10**, 135 (2020).
70. Tsugawa, H. et al. MS-DIAL: data-independent MS/MS deconvolution for comprehensive metabolome analysis. *Nat. Methods* **12**, 523–526 (2015).
71. Sumner, L. W. et al. Proposed minimum reporting standards for chemical analysis Chemical Analysis Working Group (CAWG) Metabolomics Standards Initiative (MSI). *Metabolomics* **3**, 211–221 (2007).
72. Pang, Z. et al. MetaboAnalyst 6.0: towards a unified platform for metabolomics data processing, analysis and interpretation. *Nucleic Acids Res.* **52**, W398–W406 (2024).
73. Gentleman, R., Carey, V., Huber, W. & Hahne, F. Genefilter: methods for filtering genes from high-throughput experiments. *R package version 1.64.0*. (2018).
74. Gu, Z., Eils, R. & Schlesner, M. Complex heatmaps reveal patterns and correlations in multidimensional genomic data. *Bioinformatics* **32**, 2847–2849 (2016).
75. Yurekten, O. et al. MetaboLights: open data repository for metabolomics. *Nucleic Acids Res.* **52**, D640–D646 (2024).
76. Kanehisa, M., Furumichi, M., Sato, Y., Kawashima, M. & Ishiguro-Watanabe, M. KEGG for taxonomy-based analysis of pathways and genomes. *Nucleic Acids Res.* **51**, D587–D592 (2023).

Acknowledgements

We thank all members of the Koren lab for their support, feedback, and discussions throughout this study. DB acknowledges the Israel Academy of Sciences and Humanities for supporting her PhD through a yearly scholarship from the Adams Fellowships Program.

Author contributions

D.B., S.T., and O.K. designed the study; D.B. and N.A. performed mouse experiments and data acquisition, D.B. and R.S. analyzed the data; D.B., S.T., and O.K. interpreted the results, prepared the figures, and were involved in writing and critically revising the manuscript; O.K. supervised the project. All authors approved the final version of the manuscript.

Competing interests

OK serves as an EIC of this journal and had no role in the peer-review or decision to publish this manuscript. All other authors declare no competing interests.

Additional information

Supplementary information The online version contains supplementary material available at <https://doi.org/10.1038/s41522-025-00811-w>.

Correspondence and requests for materials should be addressed to Omry Koren.

Reprints and permissions information is available at <http://www.nature.com/reprints>

Publisher's note Springer Nature remains neutral with regard to jurisdictional claims in published maps and institutional affiliations.

Open Access This article is licensed under a Creative Commons Attribution-NonCommercial-NoDerivatives 4.0 International License, which permits any non-commercial use, sharing, distribution and reproduction in any medium or format, as long as you give appropriate credit to the original author(s) and the source, provide a link to the Creative Commons licence, and indicate if you modified the licensed material. You do not have permission under this licence to share adapted material derived from this article or parts of it. The images or other third party material in this article are included in the article's Creative Commons licence, unless indicated otherwise in a credit line to the material. If material is not included in the article's Creative Commons licence and your intended use is not permitted by statutory regulation or exceeds the permitted use, you will need to obtain permission directly from the copyright holder. To view a copy of this licence, visit <http://creativecommons.org/licenses/by-nc-nd/4.0/>.

© The Author(s) 2025